TOW-PATH BASED MODELING OF WRINKLING DURING THE AUTOMATED FIBER PLACEMENT PROCESS

Roudy Wehbe, Brian F. Tatting, Ramy Harik, and Zafer Gürdal
University of South Carolina, Ronald E. McNair Center, Columbia, SC 29201, U.S.A.

Allen Halbritter and Steven Wanthal
The Boeing Company

ABSTRACT

Investigation of wrinkling within an arbitrary path for a composite tow constructed using the automated fiber placement process is presented. Governing equations and assumptions for a basic zeroth-order model are derived based on geometric considerations only, neglecting the elastic properties of the material, and formulated for an arbitrary curve on a general three-dimensional surface. A simple form of the wrinkled shape is assumed and applied to the inner edge of tow path, which might be steered tow on a smooth part surface or a straight path on complex doubly-curved part. The formulation is further simplified to describe the special case of a tow-path on a flat plate. A numerical solution is implemented within Mathematica to visualize the curved paths and to indicate potential regions for wrinkling on the surface. Several examples are presented to demonstrate the capability, including constant angle paths on a double-curved surface and curved paths on a flat surface.

1. INTRODUCTION

The usage of carbon fiber composites in large aerospace parts has pushed the industry for automation over hand layup to increase productivity and reduce cost. To answer the higher demand in composites manufacturing, Automated Fiber Placement (AFP) is being used due to its ability to manufacture complex shapes. However, the quality of the final part may be undermined by a number of defects that can be induced during the manufacturing process such as wrinkling, tow twisting, folding, missing tows, and others [1]. Based on the severity of the defect, the part might be used as is, repaired, or totally discarded. Some of these defects can be tracked up to the design phase, however others might occur due to material variability or other unknown factors.

As for wrinkling, or sometime referred as out-of-plane buckling, the main reason for its occurrence is the mismatch in length between the prescribed path on the surface and the actual delivered tow from the machine head. This mismatch in length can be detected during the design phase, hence the possibility of improvement. [2] reported that tow wrinkling occurs on the inside radius of the tow if the compressive forces are too high, and tow pull-up (or folding) occurs on the outside radius of the tow due to tensile forces. From a geometric perspective, a positive differential length (the difference between the fed tow and the actual path) will lead to tow wrinkling, whereas a negative differential length will lead to tow straightening (width reduction) or tow folding.

For flat plates, the mismatch in length can occur while steering, which is necessary to fabricate variable stiffness laminates using AFP. However, for doubly curved surfaces, the length of the two edges of the tow-path is usually not the same, even for the “straightest paths”, or mathematically

referred as geodesic paths. Hence, analyzing these surfaces for possible regions of wrinkling is necessary prior to manufacturing.

Modeling tow wrinkling is a complex task that involves process parameters (temperature, pressure and speed), material properties (viscoelastic behavior and tackiness), and geometry. Literature exists that applies the methods of stability analysis of rectangular plate-like composites with appropriate boundary conditions under loads and deformations. For example, modeling of buckling has been studied in [3], as applied to slit-tape during automated fiber placement manufacturing to establish the critical radius at which tow wrinkling occurs. Similarly, [4] used the same physical foundation to find a closed form solution for the critical steering radius in automated dry fiber placement by assuming a cosine shape function. Experimental validation for these models is difficult, since the boundary conditions assumed in the models is difficult to establish, in particular based on the lack of information on the tackiness of the foundation which is a complex parameter to calculate.

In this paper, the stability analysis based on finite size plate-like element assumption is abandoned in favor of a functional form of the tow-path with finite width. In addition, the effects of the process parameters, the viscoelasticity of the material, the tackiness of the tow with respect to its underlying surface, and the elastic properties of the tows are ignored. This first attempt is termed zeroth order solution and assumes that the deformation can be approximated purely through geometric concerns involving the shape and amplitude of the wrinkled tow.

In some sense, the slit-tape or fiber tow is approximated by a finite-width ribbon with infinitely large in–plane stiffnesses and negligible bending stiffness. Relevant geometric equations are derived and presented in the following section for a general three-dimensional surface, as well as a simplified version for a flat surface. A numerical solution is developed within a *Mathematica* program [5] and several examples are shown in the Results section including paths on a doubly curved NURBS surface, and curved path on a flat surface.

2. TOW-PATH MODELING ON GENERAL SURFACE

This section presents the relevant geometrical parameters for wrinkling analysis on a general surface. Those parameters are the surface and its corresponding tangent and normal vectors, the relevant path on the surface, its tangent, normal and bi-normal vectors, its geodesic curvatures, computing parallel curves on the surface, and the assumed shape function of the wrinkles.

2.1 Surface Definition

A general three-dimensional surface is represented through surface parameters (u, v) such that:

$$\boldsymbol{S}(u,v) = X(u,v)\hat{\imath} + Y(u,v)\hat{\jmath} + Z(u,v)\hat{k} \quad , \qquad [1]$$

where the coefficient functions (X, Y, Z) are defined for each unit vector in three-dimensional Cartesian coordinates. Once the surface is defined, an orthonormal frame on that surface can be defined using the two tangent vectors and the normal vector in the u and v directions. The tangent vectors along the surface parameters u and v are denoted by $\boldsymbol{S_u}$ and $\boldsymbol{S_v}$, and are given by:

$$\boldsymbol{S_u}(u,v) = \frac{\partial \boldsymbol{S}(u,v)}{\partial u} \quad , \quad \boldsymbol{S_v}(u,v) = \frac{\partial \boldsymbol{S}(u,v)}{\partial v}, \qquad [2]$$

where the subscripts represent differentiation with respect to those variables. These vectors are often normalized to produce unit vectors in the surface directions:

$$\widehat{\boldsymbol{S}}_{\boldsymbol{u}}(u,v) = \frac{\partial \boldsymbol{S}(u,v)/\partial u}{\|\partial \boldsymbol{S}(u,v)/\partial u\|} \quad , \quad \widehat{\boldsymbol{S}}_{\boldsymbol{v}}(u,v) = \frac{\partial \boldsymbol{S}(u,v)/\partial v}{\|\partial \boldsymbol{S}(u,v)/\partial v\|} \, , \tag{3}$$

where the operator $\|\cdot\|$ denotes the Euclidean norm and the hat symbol $\widehat{\ }$ signifies a unit vector. The unit normal vector to the surface is defined as the cross product between the surface tangents and represents the third vector of the orthonormal frame for a surface:

$$\widehat{\boldsymbol{N}}(u,v) = \frac{\boldsymbol{S_u} \times \boldsymbol{S_v}}{\|\boldsymbol{S_u} \times \boldsymbol{S_v}\|} \quad \text{or} \quad \widehat{\boldsymbol{N}}(u,v) = \widehat{\boldsymbol{S_u}} \times \widehat{\boldsymbol{S_v}} \, . \tag{4}$$

For distance calculations on the surface, the infinitesimal distance between two points $\boldsymbol{P}(u,v)$ and $\boldsymbol{P}(u+\Delta u\,, v+\Delta v)$ on the surface is given by:

$$ds^2 = E\, du^2 + F\, du\, dv + G\, dv^2 \, , \tag{5}$$

where the scalar quantities E, F and G are the first fundamental coefficients of the surface and given by:

$$\begin{aligned} E(u,v) &= \boldsymbol{S_u} \cdot \boldsymbol{S_u} \, , \\ F(u,v) &= \boldsymbol{S_u} \cdot \boldsymbol{S_v} \, , \\ G(u,v) &= \boldsymbol{S_v} \cdot \boldsymbol{S_v} \, , \end{aligned} \tag{6}$$

and the symbol " $\cdot$ " denotes the dot product.

2.2 Path Definition

The previous section defined an arbitrary surface on which the fiber tows have to be laid. An infinite number of possibilities exist for the definition of a fiber path over a general 3D surface, but the most common paths used in the literature are isoparametric curves, surface-plane intersection curves, geodesics, constant angle paths, and constant curvature paths [6,7]. In the scope of this paper only the derivation of a geodesic path will be presented since it has direct relevance to the solution process, though the formulation allows for any arbitrary definition of a path. For the definitions of the surface and path Figure 1 is used as a reference.

An arbitrary path on the surface is defined by $\boldsymbol{C}(t) = \boldsymbol{S}\big(u_c(t), v_c(t)\big)$ where $u_c(t), v_c(t) \in \Omega$, the domain of definition of the surface. The unit tangent vector to the path can be defined by:

$$\widehat{\boldsymbol{T}}(t) = \frac{d\boldsymbol{C}(t)/dt}{\|d\boldsymbol{C}(t)/dt\|} = \frac{\boldsymbol{S_u}\, du_c/dt + \boldsymbol{S_v}\, dv_c/dt}{\|\boldsymbol{S_u}\, du_c/dt + \boldsymbol{S_v}\, dv_c/dt\|} \, . \tag{7}$$

In the analysis of a path along the surface, an additional useful orthonormal frame is defined using the following three vectors: $\widehat{\boldsymbol{T}}$, the unit tangent to the path; $\widehat{\boldsymbol{N}}$, the unit normal to the surface along the path, and $\widehat{\boldsymbol{B}}$, the unit in-plane normal. This last vector $\widehat{\boldsymbol{B}}$ (often referred to as the bi-normal or bi-tangent in the literature) is tangent to the surface at a given point but orthogonal to the tangent vector along the curve. It is represented through a cross-product:

$$\widehat{\boldsymbol{B}}(t) = \widehat{\boldsymbol{N}}(t) \times \widehat{\boldsymbol{T}}(t) \, . \tag{8}$$

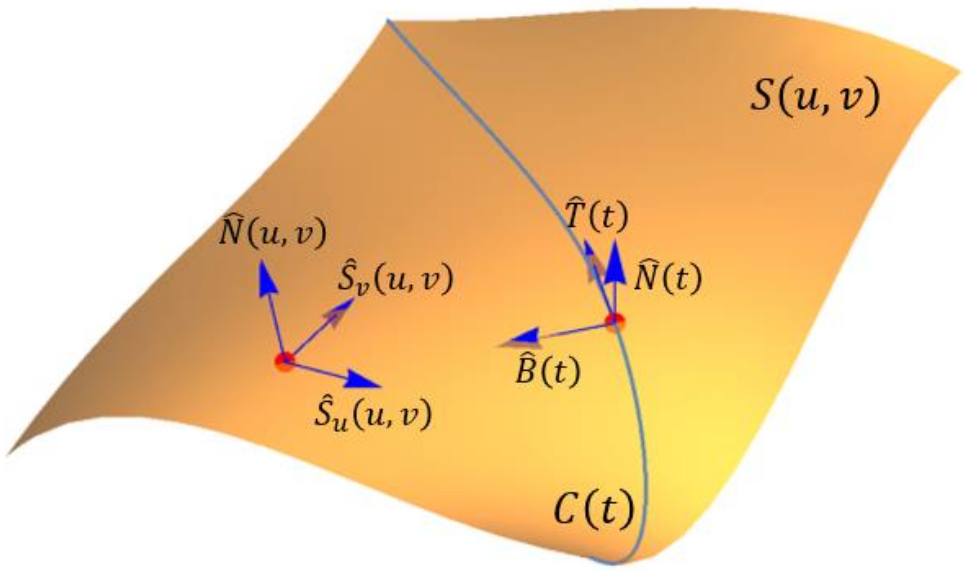

Figure 1. Surface and path definitions.

Another important feature in analyzing the path is the distance (arc length) along the path. The distance between two points on the surface along the curve $\boldsymbol{C}(t) = \boldsymbol{S}(u_c(t), v_c(t))$ can be found through integration along the path of the distance between two points on a surface from equation [5]:

$$d = \int_{t_a}^{t_b} \sqrt{E \left(\frac{du_c}{dt}\right)^2 + F \frac{du_c}{dt}\frac{dv_c}{dt} + G \left(\frac{dv_c}{dt}\right)^2}\, dt\,. \qquad [9]$$

2.3 Geodesic Path Definition and Geodesic Curvature

A geodesic path on a surface is the shortest path connecting two points on that surface. A geodesic path can also be defined starting at a point with a given direction of travel. The equations governing the path of a geodesic arise from minimization of the integral in [9] with appropriate boundary conditions, and for a general surface is calculated numerically. A geodesic path has to satisfy the following system of differential equations:

$$\begin{cases} u'' + \Gamma_{11}^1 u'^2 + 2\Gamma_{12}^1 u'v' + \Gamma_{22}^1 v'^2 = 0 \\ v'' + \Gamma_{11}^2 u'^2 + 2\Gamma_{12}^2 u'v' + \Gamma_{22}^2 v'^2 = 0 \end{cases} \qquad [10]$$

where primes ($'$) represent differentiation with respect to the parameter t and Γ_{jk}^i are the Christoffel symbols of the surface $\boldsymbol{S}$ given by:

$$\Gamma_{11}^1 = \frac{G\,E_u - 2\,F\,F_u + F\,E_v}{2(E\,G - F^2)} \quad , \quad \Gamma_{11}^2 = \frac{2\,E\,F_u - E\,E_v - F\,E_u}{2(E\,G - F^2)}$$

$$\Gamma_{12}^1 = \frac{G\,E_v - F\,G_u}{2(E\,G - F^2)} \quad , \quad \Gamma_{12}^2 = \frac{E\,G_u - F\,E_v}{2(E\,G - F^2)} \qquad [11]$$

$$\Gamma_{22}^1 = \frac{2\,G\,F_v - G\,G_u - F\,G_v}{2(E\,G - F^2)} \quad , \quad \Gamma_{22}^2 = \frac{E\,G_v - 2\,F\,F_v + F\,G_u}{2(E\,G - F^2)} \ .$$

In order to solve this system of second order differential equations, four initial conditions have to be prescribed: $u(t_0) = u_0, v(t_0) = v_0,\ u(t_1) = u_1,\ v(t_1) = v_1$ for the geodesic path between two points $\boldsymbol{P_0} = \boldsymbol{S}(u_0, v_0)$ and $\boldsymbol{P_1} = \boldsymbol{S}(u_1, v_1)$; or $u(0) = u_0, v(0) = v_0,\ u'(0) = u_0',\ v'(0) = v_0'$ for the geodesic path starting at $\boldsymbol{P_0} = \boldsymbol{S}(u_0, v_0)$ with a direction (u_0', v_0').

Lastly, several specific measures of curvature can be defined for the geometric formulation that has been defined. *Gaussian curvature K* applies to a surface and represents the intrinsic curvature of the surface at a given point. It is computed from the surface definition [1] and its derivatives. For a space curve (one not laying on a specified surface), a similar curvature parameter can be derived from the path definition $\boldsymbol{C}(t)$ and its derivatives. However, the most important estimate of curvature for the problem under consideration is referred to here as the *geodesic curvature* k_g, which measures the curvature within the tangent plane for a curve on a surface. This parameter depends on both the surface parameters and the path definition and provides a direct indication on where wrinkles might form for tow path. It is calculated as:

$$k_g = \left[\left(u_c'' + \Gamma_{11}^1 {u_c'}^2 + 2\Gamma_{12}^1 u_c' v_c' + \Gamma_{22}^1 {v_c'}^2\right) v_c' - \left(v_c'' + \Gamma_{11}^2 {u_c'}^2 + 2\Gamma_{12}^2 u_c' v_c' + \Gamma_{22}^2 {v_c'}^2\right) u_c'\right]$$

$$\times \frac{\sqrt{E\,G - F^2}}{\left(E\,{u_c'}^2 + 2\,F\,u_c' v_c' + G\,{v_c'}^2\right)^{\frac{3}{2}}} \ . \qquad [12]$$

Note that for a geodesic curve that satisfies equation [10] the geodesic curvature is identically zero, which affirms that the geodesic is the "straightest" path on a surface.

2.4 Parallel Curves on the Surface and Tow Surface

For a given base curve on the surface, parallel paths (see Figure 2) on one or both sides of the base curve have to be defined in order to show the area covered by the carbon fiber tow. Those parallel curves are computed by taking the same distance along the geodesics orthogonal to the base curve.

The algorithm to compute those curves is as follows [8]:

- Take n points $\boldsymbol{P_i}$ along the base curve: $\boldsymbol{P_i} = \{\boldsymbol{P_1}, \boldsymbol{P_2}, \dots, \boldsymbol{P_n}\}\ , i = 1 \dots n$
- Find each geodesic $\boldsymbol{G_i}$ starting at $\boldsymbol{P_i}$ in the direction orthogonal to the base curve
- Find the points $\boldsymbol{Q_i}$ on the geodesics at a distance d_i equal to the tow width
- Generate the parallel path $\boldsymbol{C_p}(t)$ by interpolating the points $\boldsymbol{Q_i}$

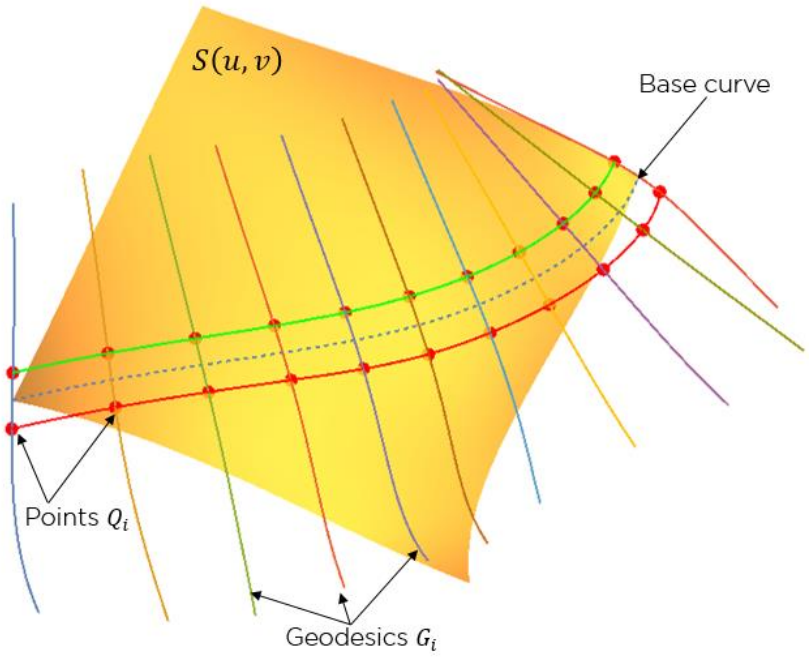

Figure 2. Parallel curves on the surface.

From these parallel path curve calculations, their lengths on the surface of a part and geodesic curvatures can be computed from equations [9] and [12], respectively.

The surface that should be covered by the tow is bounded by the initial path $\boldsymbol{C}(t)$ and the interpolated curve $\boldsymbol{C_p}(t)$. The equation of the tow surface can be generated by first creating a ruled surface $\boldsymbol{S_{tow,(u,v)}}(t,n)$ in the (u,v) domain, where $n=0$ corresponds to the initial path $\{u_c(t), v_c(t)\}$ and $n=1$ corresponds to the parallel path $\{u_p(t), v_p(t)\}$:

$$\boldsymbol{S_{tow,(u,v)}}(t,n) = \begin{Bmatrix} u_{tow}(t,n) \\ v_{tow}(t,n) \end{Bmatrix} = (1-n)\begin{Bmatrix} u_c(t) \\ v_c(t) \end{Bmatrix} + n\begin{Bmatrix} u_p(t) \\ v_p(t) \end{Bmatrix} \quad [13]$$

Then, the actual surface of the tow on the mold is generated by mapping $\boldsymbol{S_{tow,(u,v)}}(t,n)$ from (u,v) domain to the physical domain by:

$$\boldsymbol{S_{tow}}(t,n) = \boldsymbol{S}(u_{tow}(t,n), v_{tow}(t,n)) \quad [14]$$

2.5 Assumed Shape of Wrinkled Tow

The previous sections provided the necessary equations to calculate lengths and curvatures of prescribed paths and their parallel curves on a general surface. For paths with non-zero geodesic curvatures, the relative lengths of the inner and outer edges of a tow with a finite width will differ on the surface of a part. The AFP hardware on the other hand dispenses tows that have equal length on both edges. The differential length on the part surface between the two edges of the tow has to be somehow absorbed through a deformation mechanism within the tow to take the excess length on one edge of the tow that has to fit onto the part surface. Here we will assume that the edge of the tow separates from the shorter edge on the surface while the tow's edge corresponding to the longer edge on the surface remains on its prescribed path. This will generate out-of-plane wrinkles along the length of the tow.

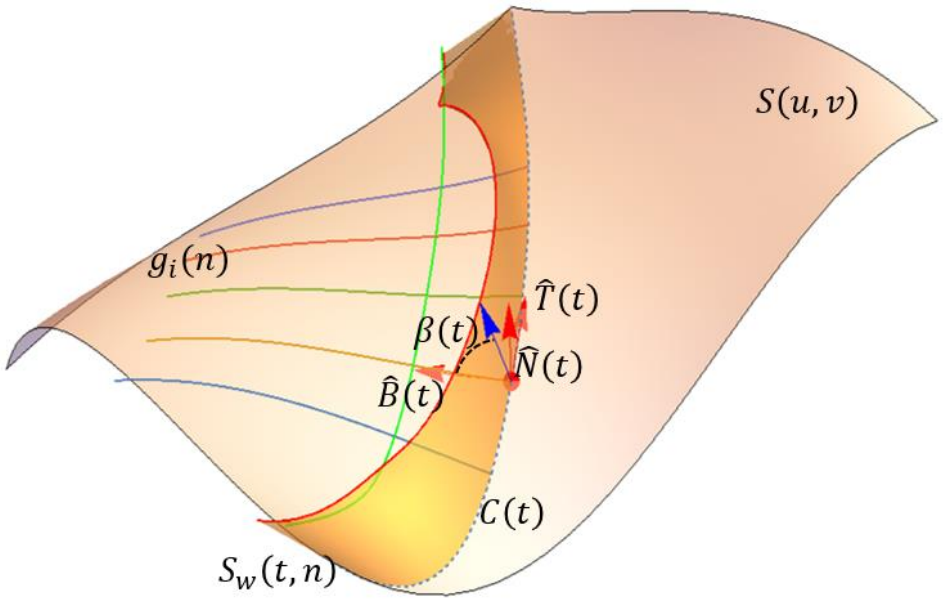

Figure 3. Schematic of a wrinkle on NURBS surface.

The wrinkled surface of the tow $\boldsymbol{S_w}(t,n)$ (see Figure 3) is derived from the tow surface $\boldsymbol{S_{tow}}(t,n)$ by the following equation:

$$\boldsymbol{S_w}(t,n) = \left(\boldsymbol{S_{tow}}(t,n) - \boldsymbol{S_{tow}}(t,0)\right) \cdot \mathcal{R}\left(\hat{T}(t), \beta(t)\right) + \boldsymbol{S_{tow}}(t,0)\,, \qquad [15]$$

where $\mathcal{R}\left(\hat{\boldsymbol{T}}(t), \beta(t)\right)$ is Rodrigues' rotation matrix corresponding to the rotation by an angle $\beta(t)$ about the axis $\hat{\boldsymbol{T}}(t)$, the unit tangent to the original path (see Appendix for details). $\beta(t)$ is assumed to have a cosine shape function and is given by:

$$\beta(t) = k\left(1 - \cos\left[\frac{2\pi(t - t_{i-1})}{t_i - t_{i-1}}\right]\right) \quad , \quad \text{for } i = 1, \dots, N \ . \qquad [16]$$

Here t_i and t_{i-1} are the starting and ending points of the tow assuming rotation-free boundary conditions at the two ends of the tow along its length at point of separation from the surface and the amplitude k is computed so that the length of the shorter edge is set equal to the length of the longer one. The integer N represents the number of wrinkling waves along the tow (the mode shape). To solve the transition points between each wave (the t_i locations), the length L is divided into N segments and the transition points are found from equation [9] based on the initial curve, such that:

$$\int_{t_{i-1}}^{t_i} \sqrt{E\left(\frac{du_c}{dt}\right)^2 + F\,\frac{du_c}{dt}\,\frac{dv_c}{dt} + G\left(\frac{dv_c}{dt}\right)^2}\, dt = \frac{L}{N} \quad , \quad \text{for } i = 1, \dots, N\,. \qquad [17]$$

Note that for $N = 1$ the end points are equal to the start and end of the curve $\boldsymbol{C}(t)$. To calculate the amplitude k of the cosine shape function, the equation for the parallel curve at a distance $n = 1$ in equation [15] is computed and inserted into the length calculation of equation [17] and an

iterative method is used until the total length of the shorter parallel curve is equal to the length of the longer one.

2.6 Simplification for Flat Surface

To provide a realistic example and verification with actual experiments for tow wrinkling, the previous equations are simplified for a flat surface. The equation for the surface [1] can be represented in three-dimensional space as:

$$\boldsymbol{S}(u,v) = u\hat{\imath} + v\hat{\jmath}\,. \tag{18}$$

Computations of the ensuing equations leads to the following relevant equations for the surface:

$$\begin{gathered} \widehat{\boldsymbol{S}}_{\boldsymbol{u}}(u,v) = \hat{\imath} \quad , \quad \widehat{\boldsymbol{S}}_{\boldsymbol{v}}(u,v) = \hat{\jmath}\,, \\ E = 1 \quad , \quad F = 0 \quad , \quad G = 1 \quad , \quad \text{All } \Gamma^{i}_{jk} = 0\,. \end{gathered} \tag{19}$$

The normal, tangent, and in-plane normal vectors become:

$$\widehat{\boldsymbol{N}}(u,v) = \hat{k} \quad , \quad \widehat{\boldsymbol{T}}(t) = \hat{u}_c'(t)\hat{\imath} + \hat{v}_c'(t)\hat{\jmath} \quad , \quad \widehat{\boldsymbol{B}}(t) = -\hat{v}_c'(t)\hat{\imath} + \hat{u}_c'(t)\hat{\jmath}\,, \tag{20}$$

with $\hat{u}_c'(t) = \frac{u_c'(t)}{\sqrt{u_c'^{\,2}(t)+v_c'^{\,2}(t)}}$, and $\hat{v}_c'(t) = \frac{v_c'(t)}{\sqrt{u_c'^{\,2}(t)+v_c'^{\,2}(t)}}$.

The equations for a geodesic path reduce to a simple system of separable ODE's, reaffirming that the shortest path on a flat surface is a straight line:

$$\begin{cases} u'' = 0 \\ v'' = 0 \end{cases} \xrightarrow{\;yields\;} \begin{cases} u(t) = c_0 t + c_1 \\ v(t) = c_2 t + c_3 \end{cases}. \tag{21}$$

The parallel edge curves can be stated more simply as:

$$\boldsymbol{C}(t) : \begin{cases} x(t) = u_c(t) \\ y(t) = v_c(t) \end{cases} \quad , \quad \boldsymbol{C_p}(t) : \begin{cases} x_p(t) = u_c(t) - w\,\hat{v}_c'(t) \\ y_p(t) = v_c(t) + w\,\hat{u}_c'(t) \end{cases}, \tag{22}$$

and the in-plane curvature is calculated from:

$$k_g(t) = \frac{u_c' v_c'' - u_c'' v_c'}{\left(u_c'^{\,2} + v_c'^{\,2}\right)^{3/2}}\,. \tag{23}$$

The assumed shape of the deformed surface is represented as:

$$\boldsymbol{S_w}(t,n) = \boldsymbol{C}(t) + n\,w\left[\cos\big(\beta(t)\big)\,\widehat{\boldsymbol{B}}(t) + \sin\big(\beta(t)\big)\widehat{\boldsymbol{N}}(t)\right]. \tag{24}$$

Lastly, the length calculations for the edges are found from:

$$\int_{t_{i-1}}^{t_i} \sqrt{\left(\frac{dx_0}{dt}\right)^2 + \left(\frac{dy_0}{dt}\right)^2}\,dt = \int_{t_{i-1}}^{t_i} \sqrt{\left(\frac{dx_d}{dt}\right)^2 + \left(\frac{dy_d}{dt}\right)^2 + \left(\frac{d\,z_d}{dt}\right)^2}\,dt = \frac{L}{N} \quad i = 1, N\,. \tag{25}$$

3. RESULTS

This section will present a direct application of the equation presented in the previous section for both a general NURBS surface and for a flat surface.

3.1 Curves on a General Surface

The first step in the analysis of a 3D towpath is to specify the surface on which the tow is laid down. To do so, the NURBS form of a surface is used since it is compatible with and implemented in most CAD software packages and offers a wide flexibility for the user. A NURBS surface is given by:

$$\boldsymbol{S}(u,v) = \frac{\sum_{i=0}^{n}\sum_{j=0}^{m} N_{i,p}(u)\, N_{j,q}(v) w_{i,j} P_{i,j}}{\sum_{i=0}^{n}\sum_{j=0}^{m} N_{i,p}(u)\, N_{j,q}(v) w_{i,j}}. \qquad [26]$$

The $P_{i,j}$ are the control points (control net), $w_{i,j}$ are the corresponding weights, $N_{i,p}(u)$ and $N_{j,q}(v)$ are the non-uniform rational B-Splines basis functions of degree p and q, respectively, which are defined over the knot vectors U and V (see [9] for details on NURBS parameterization).

To illustrate the calculation presented previously, a quasi-random NURBS surface (Figure 4) is considered with the following parameters:

$$P_{i,j} = \begin{Bmatrix} \{\{1,1,-0.643\},\{1,2,-0.404\},\{1,3,-0.795\},\{1,4,-0.513\}\}, \\ \{\{2,1,0.692\},\{2,2,0.281\},\{2,3,-0.458\},\{2,4,-0.14\}\}, \\ \{\{3,1,0.085\},\{3,2,0.986\},\{3,3,-0.693\},\{3,4,0.678\}\}, \\ \{\{4,1,0.502\},\{4,2,-0.999\},\{4,3,0.804\},\{4,4,0.475\}\} \end{Bmatrix} \qquad [27]$$

$$w_{i,j} = \{\{1,1,1,1\},\{1,1,1,1\},\{1,1,1,1\},\{1,1,1,1\}\}$$

$$\boldsymbol{U} = \boldsymbol{V} = \{0\,,0\,,0\,,0\,,1\,,1\,,1\,,1\} \quad , \quad p = q = 3$$

The *Z*-coordinate of the control points is a randomly generated real number, whereas the *X* and *Y* coordinates are equally spaced to form a square mesh between 1 and 4 (units). The knot vectors are uniform, and the weights are equal to 1. In this case, the NURBS surface is a special case of a B-Spline surface. This case is used for demonstration purpose and is displayed in Figure 4.

The path to be analyzed is chosen to have the following parameters: $u_c(t) = \sin\frac{\pi}{2}t$, $v_c(t) = t$, therefore, the path has the following equation: $\boldsymbol{C}(t) = \boldsymbol{S}(\sin\frac{\pi}{2}t\,, t)$. Calculation of the geodesic curvature [12 along the length of this curve on the NURBS surface is shown in Figure 5.

Inspection of the geodesic curvature indicates that the amplitude of the wrinkles will be higher in the first section of the path and lower in the later section. The first four mode shapes generated by the software are shown in Figure 6 which agrees with the prediction that the wrinkles are proportional to the geodesic curvature.

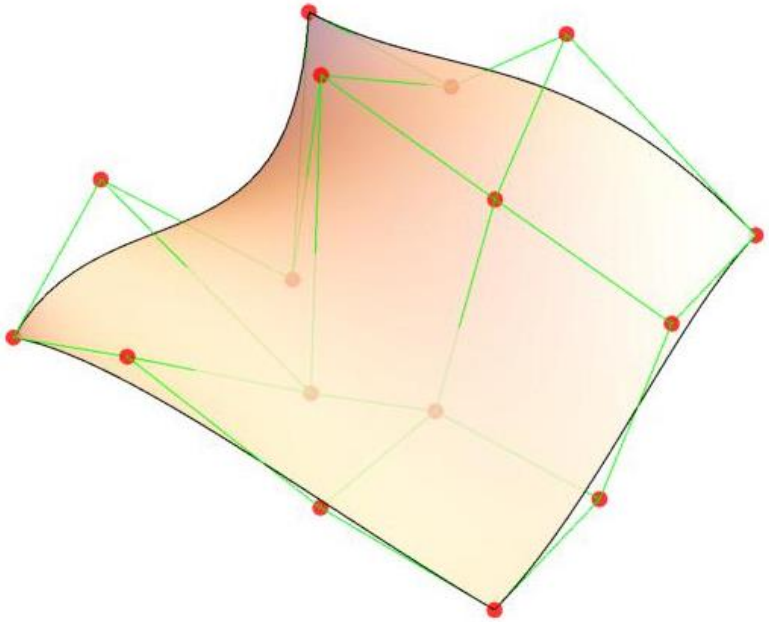

Figure 4. Example NURBS surface.

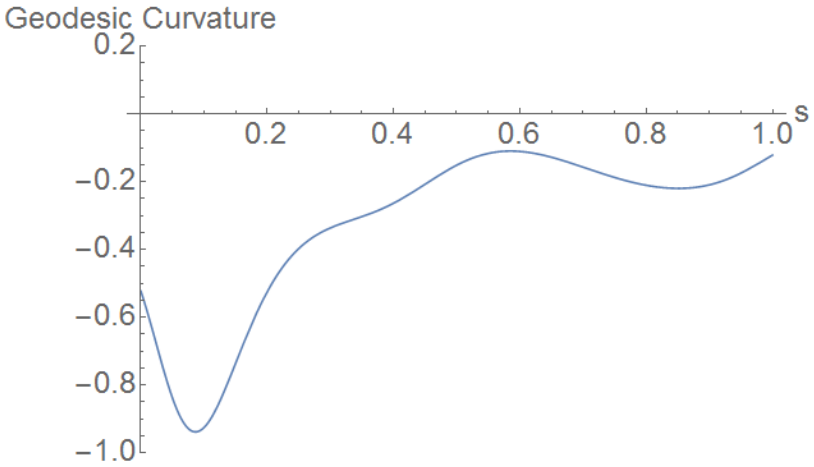

Figure 5. Geodesic curvature of the path: $\boldsymbol{C}(t) = \boldsymbol{S}\left(sin\frac{\pi}{2}t\,, t\right)$) .

Another feature that this method can offer is a general color map of the tows indicating the locations where wrinkles might appear and their severity, as demonstrated in Figure 7**Error! Reference source not found.**. Based on the differential length between the two sides of the tow (directly related to the geodesic curvature), the calculations can be used to detect the possible location of the wrinkle. A positive differential length (colored in blue) indicates that wrinkles might appear on the dashed blue side of the represented tow, whereas a negative differential length (colored in yellow-red) indicates that the wrinkles might appear on the solid orange side of the tow. The green region is the best from manufacturing perspective since it is the least portion where wrinkling defect might appear.

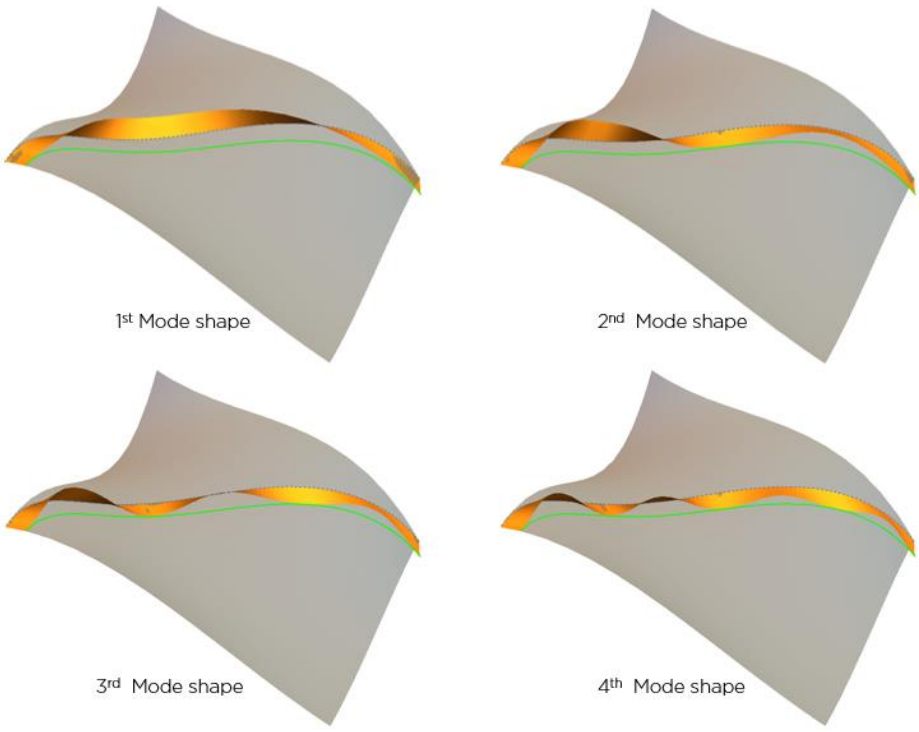

Figure 6. First four mode shapes of the tow placed on a 3D surface.

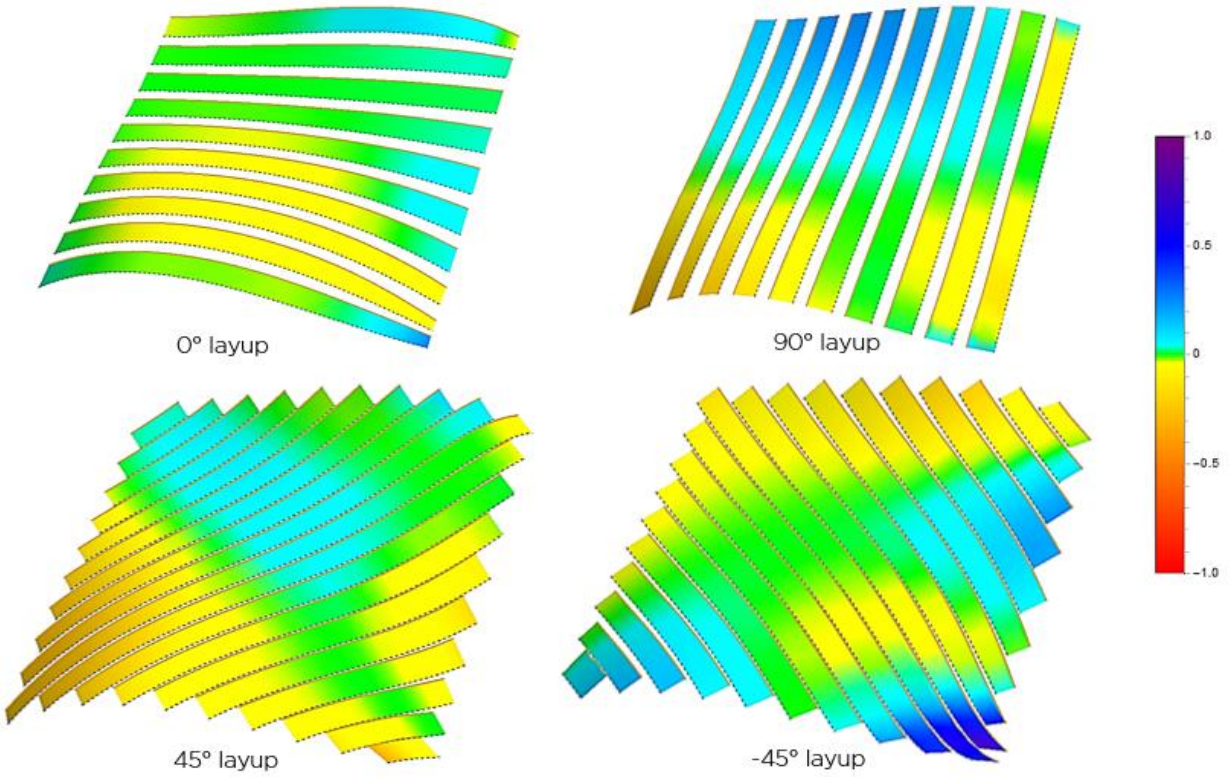

Figure 7. Differential length color map for different layup on 3D NURBS surface.

3.2 Curves on Flat Surface

Two different examples are shown in this section: the first one consists of a simple arc circle defined in parametric form, and the second one consists of a random curvilinear path defined in NURBS form. *Mathematica* [5] is used to solve the equations presented in the previous section and graphically display the deformed shape of a single tow.

3.2.1 Example 1: Circular Path

The following circular path is defined by:

$$\boldsymbol{C}(t) = \{\cos t\,, \sin t\} \quad , \quad 0 \le t \le \pi/2 \qquad [28]$$

and a tow width of $w = 0.1$ (non-dimensional units). The curvature of this path is $\kappa(t) = 1$ and the corresponding tangent and in-plane normal vectors are:

$$\widehat{\boldsymbol{T}}(t) = \{-\sin t\,, \cos t\} \quad , \quad \widehat{\boldsymbol{B}}(t) = \{-\cos u\,, -\sin u\}\,. \qquad [29]$$

The methodology is used to generate the first 4 possible mode shapes, which are shown in Figure 8.

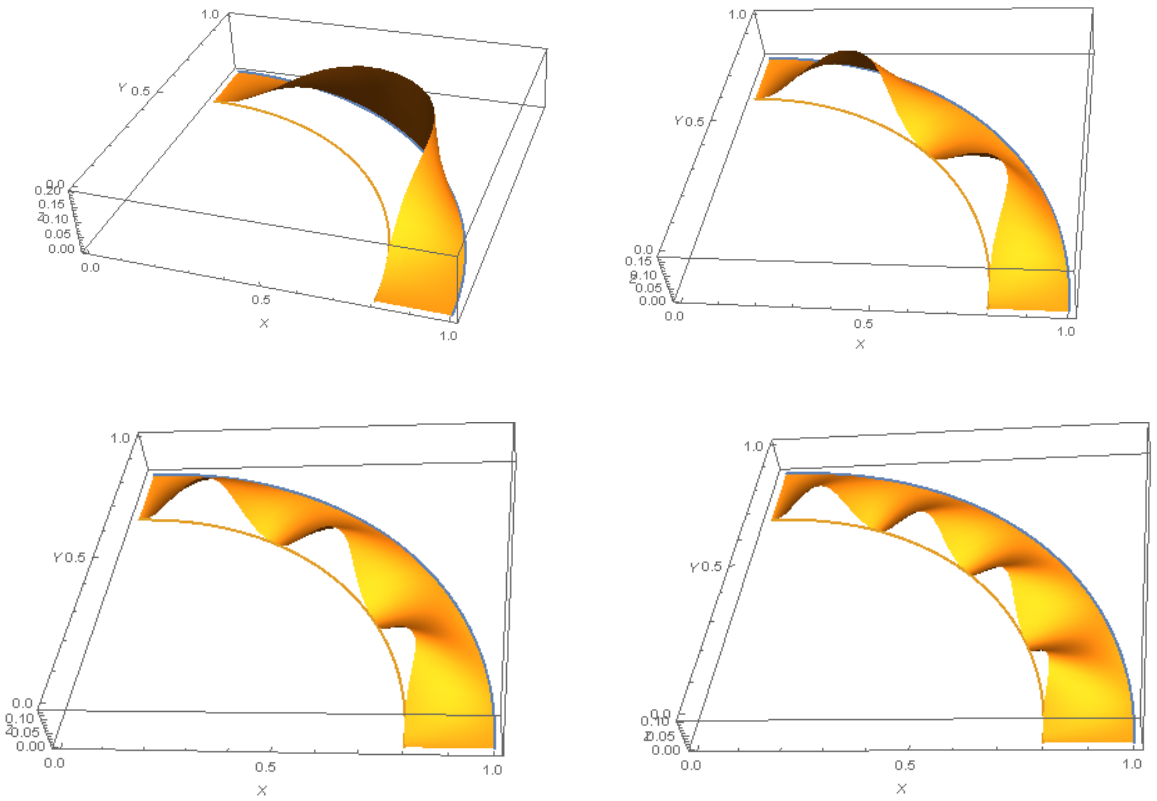

Figure 8. Deformed tow placed on a circular path: 4 different mode shapes.

Note that the amplitude of the wrinkles is affected by the mode shape. With higher mode shape the amplitude of the wrinkles decreases significantly. In addition, within a mode shape the amplitude of the wrinkles for this case is the same; i.e. the three wrinkles in the 3rd mode shape have the same amplitude, similarly for the four wrinkles in the 4th mode shape. This is due to the

fact that this circular path has a constant curvature of $k_g = 1$ and constant width $w = 0.1$ leading to a constant differential length.

3.2.2 Example 2: NURBS Path

A NURBS curve $C(t)$ is defined by a set of control points P_i and corresponding weights w_i, a degree p, and a knot vector KV. A parametrization of the NURBS curve can be obtained using the following equation:

$$C(t) = \frac{\sum_{i=0}^{n} N_{i,p}(t)\, w_i \vec{P}_i}{\sum_{i=0}^{n} N_{i,p}(t)\, w_i}, \qquad [30]$$

where $N_{i,p}(t)$ are the p^{th}-degree B-spline basis function defined on the non-uniform knot vector KV. NURBS curves are implemented in this tool because they can capture the details of the geometry, they offer more flexibility than other types of curves and they are used in most CAD tools.

A random curvilinear path is defined in NURBS form with the following parameters:

$$\begin{aligned} P_i &= \{(0,0),(2,-1),(5,-1),(4,7)\}, \\ w_i &= \{1, 1.5, 1, 1\}. \\ KV &= \{0,0,0,0,1,1,1,1\} \\ p &= 3 \quad \text{and} \quad w = 0.5 \end{aligned} \qquad [31]$$

The resulting parametric equations of the curve using [31 is:

$$C(t) = \begin{cases} x_0(t) = \dfrac{t\left(6 - 2\,t - \frac{4}{3}\,t^2\right)}{\left(\frac{2}{3} + t - 2\,t^2 + t^3\right)} \\ y_0(t) = \dfrac{t\left(-3 + 4\,t + \frac{11}{3}t^2\right)}{\left(\frac{2}{3} + t - 2\,t^2 + t^3\right)} \end{cases}. \qquad [32]$$

The results of the first four mode shapes are shown in Figure 9.

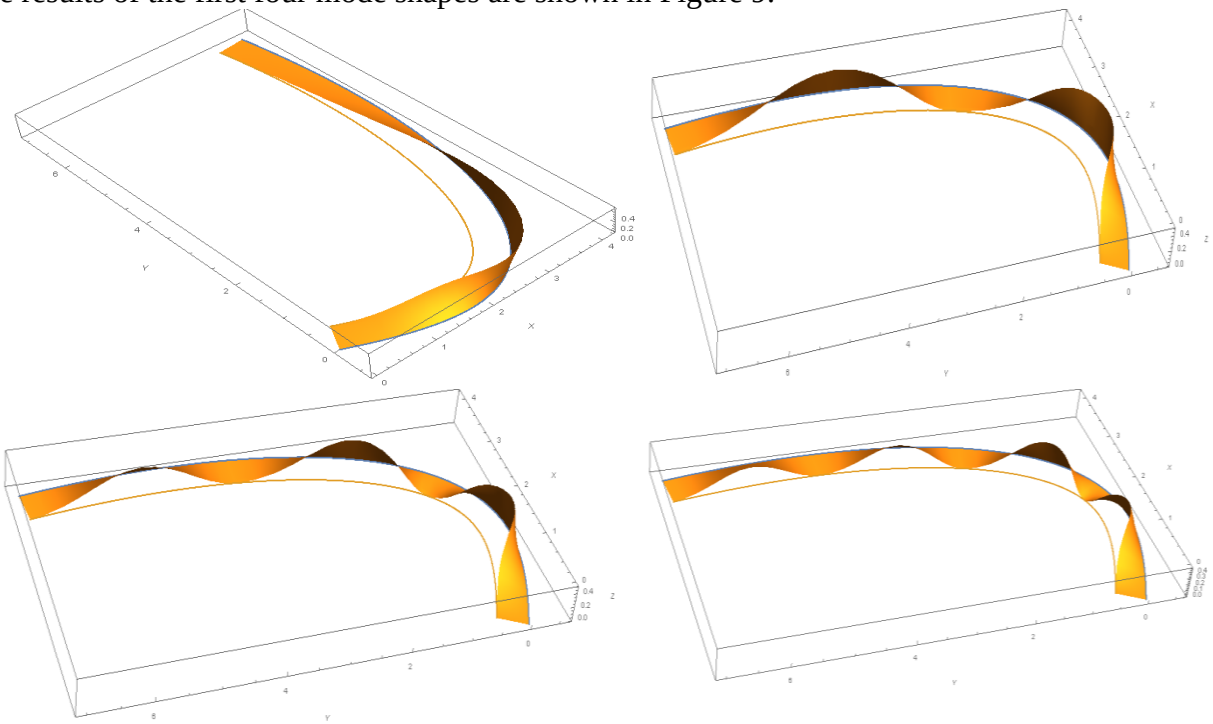

Figure 9. Tow placed on a curvilinear path in NURBS form.

Similar conclusions as earlier can be drawn from the figure above: the amplitude of the wrinkles depends on the mode shapes. In addition, it can be seen that the amplitude also depends on the curvature of the path. For instance, the portion where the path is highly curved shows the higher amplitude of the wrinkle.

4. CONCLUSIONS

A formulation for an arbitrary towpath on a general surface is developed and implemented in a computational environment to calculate the possible location of wrinkles. Based on the surface parameters and path parameters, the critical locations of the wrinkles can be determined based on the geodesic curvature of the path and the results are shown in a colored map. In addition, the shape of the wrinkle is assumed to be a cosine function similar to the clamped beam solution and an example problem is shown for demonstration. The obtained amplitude of the wrinkled tow is proportional to the geodesic curvature of the path.

The formulation is further simplified for the special case of a flat surface where the geodesic curvature is the in-plane 2D curvature and the geodesic path is a straight line. Similar conclusions to the general surface formulation are obtained.

5. ACKNOWLEDGEMENTS

The authors at the McNAIR Center would like to thank The Boeing Company for their support of this work. This research was performed under contract SSOW-BRT-W0915-0006 through the University of South Carolina and has been released for publication by The Boeing Company under approval number 17-00258-CORP.

6. APPENDIX

Rodrigues' rotation formula $\mathcal{R}(\hat{\omega}, \theta)$ computes the rotation by an angle θ about the unit axis $\hat{\omega} = (\omega_x, \omega_y, \omega_z)$ and is given by:

$$\mathcal{R}(\hat{\omega}, \theta) = e^{\tilde{\omega}\theta} = I + \tilde{\omega}\sin\theta + \tilde{\omega}^2(1 - \cos\theta) \quad [33]$$

Or in matrix form:

$$\mathcal{R}(\hat{\omega}, \theta) = \begin{pmatrix} \cos\theta + \omega_x^2(1-\cos\theta) & -\omega_z\sin\theta + \omega_x\omega_y(1-\cos\theta) & \omega_y\sin\theta + \omega_x\omega_z(1-\cos\theta) \\ \omega_z\sin\theta + \omega_x\omega_y(1-\cos\theta) & \cos\theta + \omega_y^2(1-\cos\theta) & -\omega_x\sin\theta + \omega_y\omega_z(1-\cos\theta) \\ -\omega_y\sin\theta + \omega_x\omega_z(1-\cos\theta) & \omega_x\sin\theta + \omega_y\omega_z(1-\cos\theta) & \cos\theta + \omega_z^2(1-\cos\theta) \end{pmatrix} \quad [34]$$

Where I is the 3×3 identity matrix, and $\tilde{\omega}$ is the cross product matrix of the vector $\hat{\omega}$ given by:

$$\tilde{\omega} = \begin{pmatrix} 0 & -\omega_z & \omega_y \\ \omega_z & 0 & -\omega_x \\ -\omega_y & \omega_x & 0 \end{pmatrix} \quad [35]$$

7. REFERENCES

1. Czaja, Kris. "Automated Composite Structure Inspection System." *Defense Manufacturing Conference.* Denver CO, November 28 - December 1, 2016.
2. Lukaszewicz, D. H.-J.,Ward, C. & Potter, K. D., "The engineering aspects of automated prepreg layup: History, present and future." *Composites: Part B* 43 (2012): 997-1009.
3. Beakou, A., Cano, M. & Le Cam, J. B., "Modeling slit tape buckling during automated prepreg manufacturing: A local approach." *Composite Structure* 93 (2011): 2628-2635.
4. Matveev, M. Y. , Shubel, P. J., Long, A. C. & Jones I. A., "Understanding the buckling behavior of steered tows in Automated Dry Fibre Placement." *Composites: Part A* 90 (2016): 451-456.
5. Wolfram Research, Inc., Mathematica, Version 11.0, Champaign, IL, 2016.
6. Blom, A. W., Tatting, B. F., J. M. Hol and Z. Gürdal, "Fiber path definitions for elastically tailored conical shells." *Composites: Part B* 40 (2009): 77-84.
7. Bijan, S., Gary, C., Denny, O., Gursel, A. & Ang Jr, M. H. "Trajectory generation for open-contoured structures in robotic fibre placement." *Robotics and Computer-Integrated Manufacturing* 23 (2007): 380-394.
8. Galvez, A., Iglesias, A. & Puig-Pey, J. "Computing parallel curves on parametric surfaces." *Applied Mathematical Modelling* 38 (2012): 2398-2413.
9. Piegl, L. & Wayne, T. *The NURBS Book.* Springer, 1997.